Development 134, 1231-1242 (2007) doi:10.1242/dev.02797

Constitutive activation of smoothened (SMO) in mammary glands of transgenic mice leads to increased proliferation, altered differentiation and ductal dysplasia

Ricardo C. Moraes, Xiaomei Zhang, Nikesha Harrington, Jennifer Y. Fung, Meng-Fen Wu, Susan G. Hilsenbeck, D. Craig Allred and Michael T. Lewis*

The hedgehog signaling network regulates pattern formation, proliferation, cell fate and stem/progenitor cell self-renewal in many organs. Altered hedgehog signaling is implicated in 20-25% of all cancers, including breast cancer. We demonstrated previously that heterozygous disruption of the gene encoding the patched-1 (PTCH1) hedgehog receptor, a negative regulator of smoothened (*Smo*) in the absence of ligand, led to mammary ductal dysplasia in virgin mice. We now show that expression of activated human SMO (SmoM2) under the mouse mammary tumor virus (MMTV) promoter in transgenic mice leads to increased proliferation, altered differentiation, and ductal dysplasias distinct from those caused by *Ptch1* heterozygosity. SMO activation also increased the mammosphere-forming efficiency of primary mammary epithelial cells. However, limiting-dilution transplantation showed a decrease in the frequency of regenerative stem cells in *MMTV-SmoM2* epithelium relative to wild type, suggesting enhanced mammosphere-forming efficiency was due to increased survival or activity of division-competent cell types under anchorage-independent growth conditions, rather than an increase in the proportion of regenerative stem cells per se. In human clinical samples, altered hedgehog signaling occurs early in breast cancer development, with PTCH1 expression reduced in ~50% of ductal carcinoma in situ (DCIS) and invasive breast cancers (IBC). Conversely, SMO is ectopically expressed in 70% of DCIS and 30% of IBC. Surprisingly, in both human tumors and *MMTV-SmoM2* mice, SMO rarely colocalized with the Ki67 proliferation marker. Our data suggest that altered hedgehog signaling may contribute to breast cancer development by stimulating proliferation, and by increasing the pool of division-competent cells capable of anchorage-independent growth.

KEY WORDS: Hedgehog signaling, Stem cell, Progenitor cell, Invasive breast cancer, Ductal carcinoma in situ

INTRODUCTION

The hedgehog signaling network regulates pattern formation, proliferation, cell fate and stem/progenitor cell maintenance and self-renewal in many organs (Cohen, Jr, 2003; Hooper and Scott, 2005; Lewis and Veltmaat, 2004; Nusse, 2003). Genetic analyses in mice indicate a role in mammary ductal morphogenesis, and recent data suggest a role in human mammary epithelial stem cell self-renewal (Liu et al., 2006). In addition to hedgehog functions in normal development, altered hedgehog signaling is now implicated in approximately 20-25% of all cancers (Briscoe and Therond, 2005), and there is increasing evidence to suggest a role in breast cancer (Chang-Claude et al., 2003; Kubo et al., 2004; Lewis et al., 2001; Lewis et al., 1999; Liu et al., 2006; Mukherjee et al., 2006; Naylor et al., 2005). However, the specific roles hedgehog network genes play in normal mammary gland development remain unclear, and no experiments have been performed to test directly whether inappropriately activated hedgehog signaling has functional consequences for gland development, or causes breast cancer.

Development of the mouse mammary gland begins in the embryo with formation of a rudimentary ductal tree, but most development occurs after puberty (Daniel and Silberstein, 1987; Sakakura, 1987). At puberty, ovarian steroids stimulate rapid and invasive ductal elongation and branching morphogenesis. At the growing tips of elongating ducts are bulb-like structures called terminal end buds (TEBs). Histologically, TEBs consist of two highly proliferative cell compartments: an outer 'cap cell' compartment, and an inner 'body cell' compartment consisting of four to six layers of relatively undifferentiated luminal epithelial cells. As the TEB invades the mammary fat pad, cap cells serve as a progenitor cell population and differentiate into myoepithelial cells that line the basement membrane (Williams and Daniel, 1983), whereas body cells are thought to give rise to all luminal epithelial cell subtypes of the mature duct, including new multipotent mammary stem cells. As ducts elongate, they are surrounded by a periductal stroma consisting of fibroblasts, macrophages, eosinophils and vascular cells, within the confines of the mammary fat pad.

Hedgehog signaling involves two types of cells: a signaling cell expressing a member of the hedgehog family of secreted ligands [sonic hedgehog (SHH), indian hedgehog (IHH), or desert hedgehog (DHH)], and a responding cell expressing one or more patched family hedgehog receptors [patched-1 (PTCH1) and patched-2 (PTCH2)]. In the absence of ligand, PTCH1 can function to inhibit downstream signaling via the smoothened (SMO) transmembrane effector protein. Under these conditions, expression of hedgehog target genes is inhibited by repressor forms of one or more members of the Gli family of transcription factors (GLI2 or GLI3). In the presence of ligand, PTCH1 releases inhibition of SMO, which leads to induction of target genes by transcriptional activator forms of Gli transcription factors (GLI1, GLI2 or GLI3). In addition to its signal transduction activities, PTCH1 can also function to sequester hedgehog ligand, thereby restricting the range over which free ligand can signal (reviewed by

Baylor Breast Center and Department of Molecular and Cellular Biology, Room N1210; MS:BCM600, Baylor College of Medicine, One Baylor Plaza, Houston, TX 77030, USA.

*Author for correspondence (e-mail: mtlewis@breastcenter.tmc.edu)

Accepted 3 January 2007

Hooper and Scott, 2005). Finally, there is evidence to suggest that PTCH1 can function as a 'dependence receptor' to induce apoptosis in cell types dependent on ligand-bound PTCH1 for survival (Chao, 2003; Guerrero and Ruiz i Altaba, 2003; Thibert et al., 2003).

Our laboratory previously demonstrated crucial functions for *Ptch1* and *Gli2* in mammary ductal development (Lewis et al., 2001; Lewis et al., 1999; Lewis and Veltmaat, 2004). Heterozygous mutation of *Ptch1* (*ΔPtch1/+*) led to ductal dysplasia in virgin mice characterized by multiple epithelial cell layers within the ducts (Lewis et al., 1999). Similarly, transplantation rescue of whole mammary glands from homozygous *Gli2*-null mouse embryos yielded ductal dysplasias (Lewis et al., 2001). However, for both *Ptch1* and *Gli2*, transplantation of mutant epithelium into a wild-type stroma failed to recapitulate the phenotype observed in intact glands, suggesting that these two genes function primarily in the stroma to regulate epithelial cell behavior. Thus, despite developmentally regulated hedgehog network gene expression in the epithelial compartment (Lewis et al., 2001), a role for activated hedgehog signaling in the epithelium has not been demonstrated during ductal development (Gallego et al., 2002; Michno et al., 2003), and the consequences of inappropriate hedgehog signaling in the epithelium remain unknown.

Our published working model for hedgehog signaling in mammary ductal development (Lewis and Veltmaat, 2004; Lewis and Visbal, 2007) proposes that hedgehog signaling may function transiently in the body cell layer of the TEB, but that signaling must be prevented in differentiated ducts. Consistent with this hypothesis, Liu and colleagues (Liu et al., 2006) showed that treatment of human breast epithelium with recombinant hedgehog ligand increased both primary and secondary mammosphere formation [in vitro assays of anchorage-independent growth, and of self-renewal of both stem and progenitor cell types (Dontu et al., 2003; Dontu and Wicha, 2005)], whereas treatment with the hedgehog signaling antagonist cyclopamine decreased mammosphere formation. In this paper, we examine the effect of sustained SMO-mediated hedgehog signaling during ductal elongation in virgin transgenic mice, and correlate our results with altered PTCH1 and SMO expression in human breast cancer. Taken together, our results are consistent with a role for hedgehog signaling in mammary epithelial progenitor cell regulation, and suggest that ectopic hedgehog signaling may contribute to human breast cancer by stimulating proliferation, and by increasing the pool of division-competent cells capable of anchorage-independent growth.

MATERIALS AND METHODS

Generation of *MMTV-SmoM2* transgenic mice and other mouse strains

Transgenic mice expressing constitutively activated human SMO under the control of the MMTV promoter [*Tg(MMTV-SmoM2)*] were generated by the Baylor College of Medicine Mouse Embryo Manipulation Core (Dr Franco DeMayo, Director) in the inbred FVB background. The *MMTV-SmoM2* construct was a kind gift from Dr Frederick de Sauvage (Genentech, South San Francisco, CA). Mice carrying a targeted disruption allele of the *Ptch1* gene (allele $Ptch1^{tm1Mps}$) were a generous gift from Dr Matthew Scott (Stanford University, Palo Alto, CA), and were maintained by backcrossing to B6D2F1 mice. Genotype determination for the *Ptch1* disruption allele was performed as described previously (Lewis et al., 1999). Mice were maintained in accordance with the NIH Guide for the Care and Use of Experimental Animals with approval from our Institutional Animal Care and Use Committee.

Screening *MMTV-SmoM2* transgenic founder lines

Purified tail DNA from founders was used for PCR analysis for the presence of the *MMTV-SmoM2* transgene. Primers used were: forward, 5′-GAG-CTGCAGAAGCGCCTGGGCC-3′; reverse, 5′-GGTATTGGTTCCTC-TCTTTCCTG-3′. Cycling conditions were: 94°C for 35 seconds, 62°C for 40 seconds, and 72°C for 50 seconds. Detection of a ~450 bp product indicated presence of the transgene. Of seven transgenic founder lines, five yielded progeny expressing the *MMTV-SmoM2* transgene by RT-PCR.

Five female mice per genotype per line were screened at 5 and 10 weeks of age for expression of *Smo* mRNA and protein, as well as for changes in ductal patterning, histology, proliferation, apoptosis and expression of steroid hormone receptors. One line showing a representative ductal phenotype and proliferation rate [designated *Tg(MMTV-SmoM2)724Mtl*], and a line showing an identical ductal phenotype but elevated proliferation rate [designated *Tg(MMTV-SmoM2)732Mtl*] were chosen for follow-up analysis (hereafter referred to as lines 724 and 732, respectively). Unless otherwise indicated, all data shown are for line 724.

Whole gland morphological analysis

Mammary glands #1-5 were harvested from the right side of at least ten female mice at 5 and 10 weeks of age, as well as at greater than 50 weeks of age (palpated weekly after 52 weeks of age to assay for tumor development), fixed in ice-cold 4% paraformaldehyde in PBS, and examined as whole-mount preparations using a Neutral Red staining protocol. After fixation, fat was removed in three changes of acetone (1 hour each) and glands were stained in Neutral Red staining solution (0.01% Neutral Red in 100% ethanol acidified to pH 5.0 with glacial acetic acid) overnight with constant stirring. Glands were destained in two changes of 100% ethanol, cleared in two changes of xylenes (1 hour each), and stored in xylenes.

Average TEB number per gland was quantified using the #3 mammary gland at 5 weeks of age. Branch-point analysis and evaluation of retained TEB-like structures were conducted using the #3 mammary gland at 10 weeks of age by direct counting of all branch points. Phenotypic analysis of *MMTV-SmoM2* mice at other phases of gland development (e.g. pregnancy, lactation, involution) will be presented elsewhere.

Immunohistochemistry and immunofluorescence analysis

For histological analysis, the #2 and #3 mammary glands from the left side of the animal were fixed in 4% paraformaldehyde in PBS, embedded in paraffin, sectioned, and either stained with Hematoxylin-Eosin or used for immunolocalization studies. Antibodies used for immunolocalization studies are listed in Table 1. Immunostaining was performed with antigen retrieval in 0.1 M Tris-HCl (pH 9.0) with 10% Tween-20, or in TRS (DakoCytomation), by heating to 120°C for 10 minutes in a pressure cooker. For immunohistochemistry, detection was by standard peroxidase staining using the ABC system (Vector Laboratories). For immunofluorescence, sections were counterstained with DAPI in Mounting Medium (Vectashield).

Standard brightfield and immunofluorescence microscopy were performed using a Zeiss Axioskop2 Plus microscope. Deconvolution microscopy (Fig. 2) was performed using a Zeiss Axiovert S100 ZTV microscope and SoftWorX software.

Primary mammary epithelial cell isolation

Primary mammary epithelial cells were isolated from freshly dissected mammary glands by enzymatic dissociation overnight in DMEM-Ham's F12 medium (5 ml per mouse) containing collagenase (1 mg/ml), hyaluronidase (100 U/ml), penicillin-streptomycin (100 U/ml), and gentamycin (50 μg/ml), essentially as described (Smith, 1996). Resulting cell pellets were treated with 1 ml 0.25% trypsin-EDTA at 37°C for 5 minutes. Trypsin was inactivated with 10 ml HBSS containing 5% serum. Cells were centrifuged and washed three times in HBSS containing 5% serum. After the final wash, each preparation was filtered through a 40 μm strainer to yield a single-cell suspension. Single-cell suspensions were used directly in mammosphere-formation assays and limiting-dilution transplantation assays.

Mammosphere-formation and transplantation assays

Primary mammary epithelial cells derived from five paired sets of wild-type or *MMTV-SmoM2* mice (three to four mice per genotype per set) were plated in triplicate wells of six-well, ultra-low attachment plates (2 ml per well) at a concentration of 30,000 cells/ml as described previously (Chen et al., 2007; Dontu et al., 2003; Youn et al., 2005). Cells were fed every 3-4 days for 10-

Table 1. Antibodies used

Antibody	Source	Clone/catalogue number	Dilution
Estrogen receptor (ER)	Santa Cruz Biotechnology	MC-20	1:100
Progesterone receptor (PR)	Santa Cruz Biotechnology	C-19	1:800
Ki67	Dako Cytomation	MIB-1	1:1000
Cleaved caspase-3	Cell Signaling Technology	9661	1:25
Cytokeratin 6 (CK6)	Covance	PRB-169P	1:500
Patched-1 (PTCH1)	Santa Cruz Biotechnology	H-267	1:25
Smoothened (SMO)	Santa Cruz Biotechnology	N-19	1:50
Patched-1 (PTCH1)*	Santa Cruz Biotechnology	G-19	1:50
Smoothened (SMO)*	Santa Cruz Biotechnology	C-17	1:50
Smooth muscle actin (SMA)	Dako Cytomation	1A4	1:400
Donkey anti-goat	Molecular Probes	–	1:200
Donkey anti-rabbit	Molecular Probes	–	1:200

*Used on a subset of samples to confirm the expression patterns observed.

14 days. Primary mammospheres were counted for each genotype, and the percentage of mammosphere-forming cells was calculated as a measure of mammosphere-forming efficiency.

To demonstrate that mammospheres contained stem cells capable of regenerating ductal trees, single mammospheres derived from wild-type and *MMTV-SmoM2* mice were transplanted into contralateral cleared fat pads of 3-week-old recipient FVB female mice (Deome et al., 1959), and allowed to grow for 8 weeks. Glands were then excised, fixed and stained as whole-mount preparations.

Limiting-dilution cell transplantation assays

Primary mammary epithelial cells derived from five paired sets of wild-type or *MMTV-SmoM2* mice (three to four mice per genotype per set) were counted on a hemocytometer, resuspended at the desired concentration in a 1:1 solution of PBS:Matrigel (BD Biosciences, 354234), and kept on ice until transplantation. Cells of each genotype were injected at limiting dilutions (1000, 500, 200, 100, 50 and 25 cells per gland, in a total volume of 10 μl) into contralateral cleared fat pads of #4 mammary glands of 21-day-old female wild-type mice using a 25G needle attached to a 50 μl Hamilton glass syringe (Deome et al., 1959). Seven weeks after transplantation, #4 glands and a #3 host control gland were excised and stained as whole-mounts. Glands showing at least 5% fat pad filling were scored as a positive 'take'.

Human breast clinical samples

Low density tissue arrays comprising archival formalin-fixed, paraffin-embedded samples of either ductal carcinoma in situ (DCIS), invasive breast cancer (IBC), or normal tissue derived from patients with breast cancer were used. All tissue was obtained and used with approval from our Institutional Review Board. DCIS samples had been scored previously for histological grade. Both DCIS and IBC samples had been scored previously for expression of estrogen receptor alpha (ERα; ESR1 – Human Gene Nomenclature Database), ERBB2 (HER2) and p53 (TP53– Human Gene Nomenclature Database) by the method of Allred (Allred et al., 1998; Harvey et al., 1999), in which a total score (0-8) is assigned as the sum of the proportion score (0-5) and an intensity score (0-3) for the expression of a given gene.

Quantitative RT-PCR

Total RNA was extracted using Trizol Reagent (Invitrogen). Total RNA (100 ng per sample, in triplicate) was reverse-transcribed (M-MLV Reverse Transcriptase, Invitrogen) following the manufacturer's protocol. The resulting cDNA was analyzed using an Applied Biosystems 7500-Fast thermocycler for TaqMan quantitative PCR (Q-PCR) using standard conditions. TaqMan Assay On Demand primers and probes were purchased from Applied Biosystems. Product accumulation was evaluated using the comparative Ct method (ΔΔCt method), with beta-actin (*ActB*) as an endogenous control for normalization (Livak and Schmittgen, 2001).

Statistical analysis

Comparisons of gene expression levels across wild-type and transgenic lines 724 and 732 were assessed by one-way ANOVA and pairwise *t*-tests. Spearman correlation coefficients were calculated to assess associations between human SMO and the expression of mouse hedgehog network genes. Changes in hedgehog network gene expression in *ΔPtch1/+* animals relative to wild type were evaluated using a *t*-test. For protein expression analyses, the average percentage of cells expressing a given protein in a given genetic background was compared with corresponding wild-type controls using the Wilcoxon rank-sum test.

For comparison of TEB number and branch-point number between glands of wild-type versus *MMTV-SmoM2* mice, mean numbers per gland were compared using a *t*-test. Tumor incidence between wild-type and *MMTV-SmoM2* mice was compared using Fisher's exact test.

For mammosphere-formation assays, mammosphere-formation efficiency values were log-transformed and compared between paired groups of wild-type and *MMTV-SmoM2* animals using a paired *t*-test. Single mammosphere transplantation assays were performed to evaluate the frequency of mammospheres containing regenerative stem cells in wild-type versus *MMTV-SmoM2* mice. Regeneration frequencies were compared using Fisher's exact test.

Limiting-dilution analysis was performed to estimate the frequency of regenerative stem cells in primary mammary epithelial cell preparations, along with 95% Wald confidence intervals [Smyth G. (2006) Statmod: Statistical Modeling. R package version 1.2.4. http://www.statsci.org/r]. The single-hit Poisson model (SHPM) was fitted to limiting-dilution data using a complementary log-log generalized linear model (Bonnefoix et al., 1996).

In human clinical samples, correlations between expression of PTCH1 or SMO and clinically-relevant markers in DCIS, as well as the correlation between PTCH1 and SMO expression in DCIS and IBC, were tested for statistical significance using Spearman's rank correlation. All of the variables in the correlation analysis were analyzed as continuous variables. Immunohistochemical total scores for expression of PTCH1 and SMO were compared between normal, DCIS, and IBC tissues using the Wilcoxon rank-sum test. Statistical analyses were performed with SAS (version 9.1), S-PLUS (version 7.0), or R (version 2.2.1). *P* values of 0.05 or less were deemed statistically significant.

RESULTS

Ectopic SMO expression leads to mammary dysplasia in transgenic mice

Based on our working model, we hypothesized that constitutive activation of hedgehog signaling in the epithelium might lead to altered ductal development, altered differentiation, and, perhaps, tumor formation. To test these hypotheses, we generated transgenic mice expressing a constitutively activated form of human SMO (Xie et al., 1998) selectively in mammary epithelium under the control of the MMTV promoter [Tg*(MMTV-SmoM2)*].

In whole-mount analysis, glands of wild-type mice at 5 weeks of age showed normal morphology of TEBs and subtending ducts (Fig. 1A). By contrast, TEBs of *MMTV-SmoM2* mice frequently displayed excessive budding at the neck of the TEB (Fig. 1B) and an increase in TEB number (Fig. 1C) (*P*=0.05). In histological

analyses, wild-type glands showed normal TEB structure (Fig. 1D). By contrast, ~30% of TEBs in *MMTV-SmoM2* glands showed disorganized cap and body cell layers (Fig. 1E).

At 10 weeks of age, wild-type ducts showed simple patterning and duct structure (Fig. 1F). By contrast, *MMTV-SmoM2* transgenic mice showed one or more glands with enhanced side budding (Fig. 1G) and increased branching by branch-point analysis (Fig. 1H) (P=0.04). Approximately 60% of transgenic mice showed retention of TEB-like structures (Fig. 1G, inset, and Fig. 1H).

At 10 weeks of age, ducts of wild-type glands (Fig. 1I) showed normal histoarchitecture. Ducts of *MMTV-SmoM2* glands showed histology consistent with increased side-budding, but appeared normal with respect to the lumenal and myoepithelial cell layers (Fig. 1J), and did not show ducts having multiple layers of lumenal epithelium that are characteristic of *ΔPtch1/+* mice (Lewis et al., 1999) (see also Fig. 3E,F). Lumenal and myoepithelial cell layer number were confirmed by immunostaining for smooth muscle actin (SMA) (Fig. 1K,L) and p63 (not shown). Retained TEB-like structures showed histoarchitecture similar to TEBs, but the body cell layer was generally only 2-4 cell layers thick (Fig. 1J, inset).

In an interim analysis of an ongoing tumor-formation study, no tumors have been detected in a cohort of wild-type virgin mice over 52 weeks of age (n=84), or in a cohort of aged *MMTV-SmoM2* mice from line 724 (n=43). Two tumors have been detected in a cohort of *MMTV-SmoM2* mice from line 732 (n=80). However, this frequency of tumor formation is not statistically different from wild type (P=0.4). Thus, *MMTV-SmoM2* expression in virgin mice does not lead to high frequency tumor formation.

Our initial screen suggested that only a small percentage of epithelial cells in *MMTV-SmoM2* mice expressed detectable levels of SMO protein. Consistent with this observation, Q-PCR did not detect significant changes in hedgehog network gene expression, with the possible exception of decreased *Ptch1* in line 732 (see Fig. S1 in the supplementary material). Gene expression analysis in *ΔPtch1/+* mice

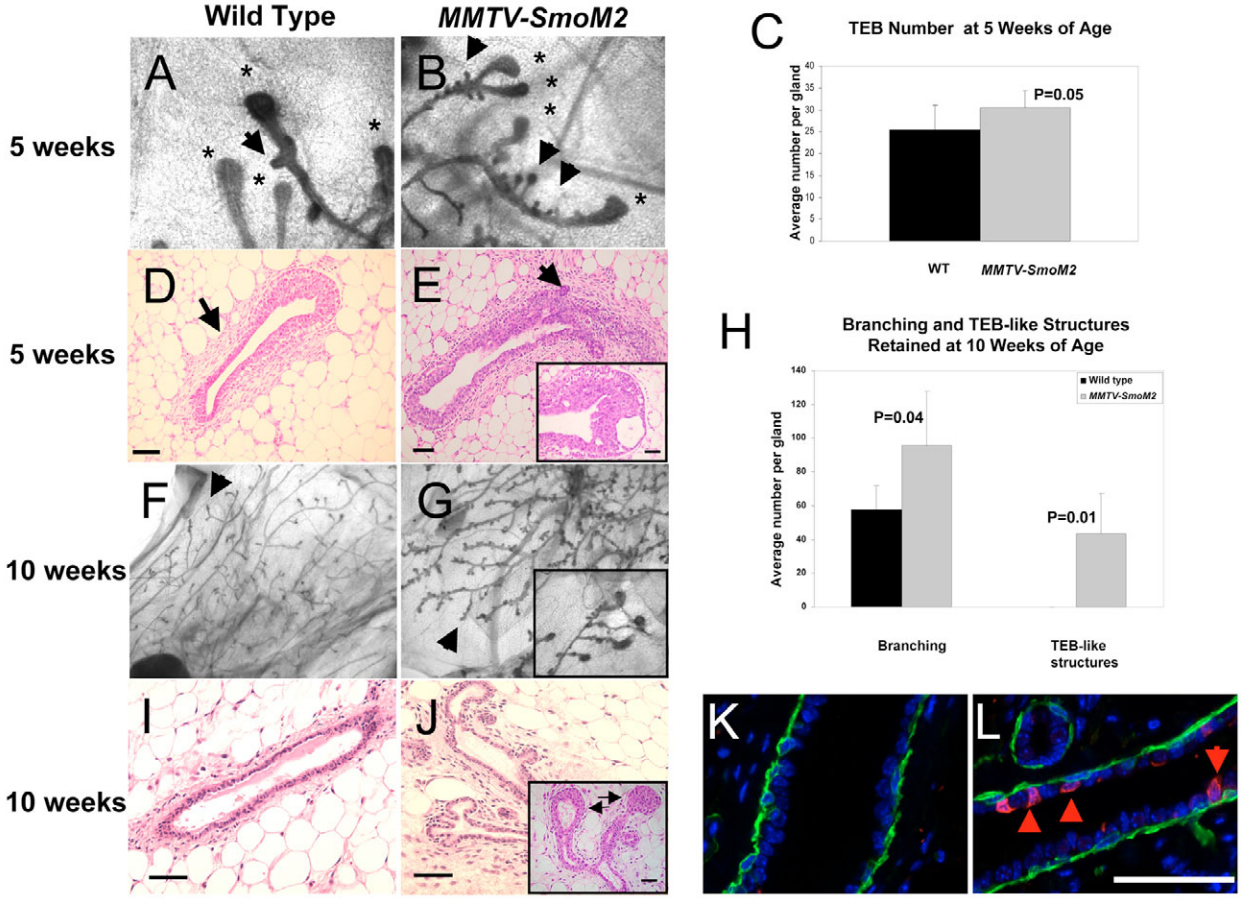

Fig. 1. Whole-mount and histological analysis of mammary glands from wild-type and *MMTV-SmoM2* mice. (**A**) Whole-mount showing a normal TEB array from a wild-type mouse at 5 weeks of age. Terminal structures are indicated with an asterisk; side-buds are arrowed. (**B**) Whole-mount showing a TEB array from an *MMTV-SmoM2* transgenic mouse at 5 weeks of age. Symbols are as described in A. (**C**) Quantification of TEB number in wild-type versus *MMTV-SmoM2* mice at 5 weeks of age. (**D**) Histological preparation of a TEB in a wild-type gland showing organized cap and body cell layers, as well as normal periductal stroma condensing around the neck of the TEB (arrow). (**E**) Histological preparation of TEB in an *MMTV-SmoM2* transgenic gland showing abnormal histology associated with the side-budding phenotype (arrow). TEBs can also show disorganized cap and body cell layers (inset). (**F**) Whole-mount from a 10-week-old wild-type mouse showing normal duct patterning and blunt-ended ducts (arrowhead). (**G**) Whole-mount from a 10-week-old *MMTV-SmoM2* mouse showing an increase in side budding and branching (arrowhead). Inset shows retained TEB-like structures. (**H**) Branch-point analysis and quantification of retained TEB-like structures at 10 weeks of age as a function of genotype. (**I**) Histological preparation of a normal mature duct in a wild-type gland. (**J**) Histological preparation of a mature duct in an *MMTV-SmoM2* gland. Inset shows retained TEB-like structures (arrows). (**K**,**L**) Dual immunofluorescence for SMO and SMA in (K) wild-type and (L) *MMTV-SmoM2* ducts. Arrowheads indicate SMO-expressing cells. Scale bars: 50 μm.

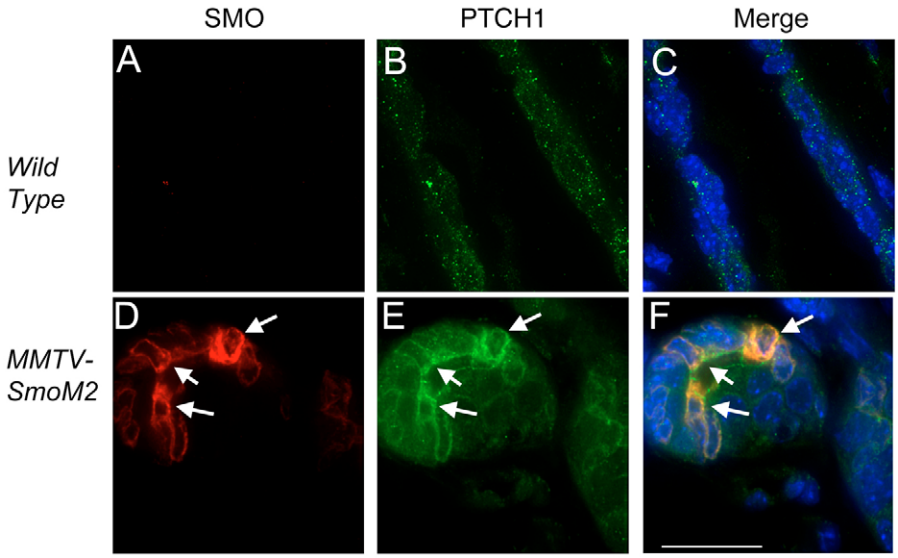

Fig. 2. Dual immunofluorescence deconvolution microscopy for SMO and PTCH1 in wild-type and *MMTV-SmoM2* transgenic mammary glands. Expression of SMO (**A**,**D**), PTCH1 (**B**,**E**) and merged three-color images including the DAPI counterstain (**C**,**F**) for wild-type (A-C) and MMTV-SmoM2 transgenic (D-F) mammary glands. (A) No detectable SMO expression. (B) Near uniform PTCH1 expression. (C) Merge of A and B. (D) Area of duct in a transgenic gland showing ectopic SMO expression. (E) PTCH1 expression in the same duct showing cell to cell variation in PTCH1 staining. (F) Merge of D and E showing (arrowed) SMO^+ cells in which PTCH1 is moderately elevated relative to SMO^- cells. Scale bar: 50 μm.

was consistent with results in *MMTV-SmoM2* mice. In *ΔPtch1/+* mice, with the exception of *Hip1*, whose expression by Q-PCR was elevated 2-fold above wild type (P=0.049), *ΔPtch1* heterozygosity was also not sufficient to induce expression of other hedgehog network genes (see Fig. S1 in the supplementary material).

Because gene expression changes in a small number of cells can be masked using mRNA or protein derived from whole mammary glands, it was necessary to evaluate transgene expression and signaling activation by dual immunofluorescence analysis for SMO and PTCH1. Elevated expression of *Ptch1* – either mRNA or protein – can be observed in response to intermediate and high levels of hedgehog network activation (Hooper and Scott, 2005).

Whereas SMO was undetectable in ducts of wild-type glands at 10 weeks of age (Fig. 2A), PTCH1 was near-uniformly detected in punctate foci in the cytoplasm of epithelial cells by deconvolution microscopy (Fig. 2B,C). In *MMTV-SmoM2* mice, ducts with altered morphology generally showed detectable SMO protein expression (Fig. 2D). Staining was mosaic, with a median of only 5.7% of all epithelial cells showing detectable SMO expression (Fig. 2F). In most SMO-expressing cells, PTCH1 expression appeared largely membrane-associated and was slightly to moderately elevated relative to adjacent SMO-negative cells, consistent with intermediate to high levels of signaling activation in SMO-positive cells (Fig. 2E,F).

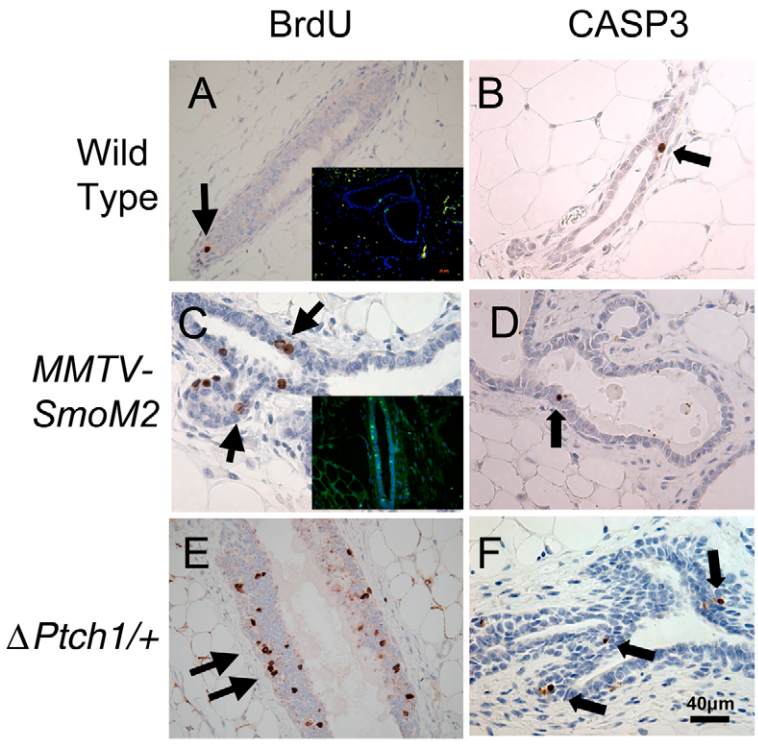

Fig. 3. Proliferation and caspase-3-mediated apoptosis as a function of genotype at 10 weeks of age. Each marker is shown at the top of the column to which it applies. Genotype of the mouse from which the gland was derived is shown to the left of the row to which it applies. Arrows highlight stained cells or regions of epithelium expressing the marker. (**A**) BrdU and Ki67 (inset) staining in wild type. (**B**) Cleaved caspase-3 staining showing rare apoptotic cells. (**C**) BrdU and Ki67 (inset) staining in an *MMTV-SmoM2* gland. (**D**) Cleaved caspase-3 staining showing a rare apoptotic cell. (**E**,**F**) BrdU and cleaved caspase-3 staining, respectively, in a *ΔPtch1/+* gland displaying the characteristic ductal phenotype.

PTCH1 loss and SMO activation increase proliferation in the mammary gland in vivo

We next compared BrdU incorporation rates and expression patterns for cleaved caspase-3, estrogen receptor (ER) and progesterone receptor (PR), using glands of 10-week-old *MMTV-SmoM2*, *ΔPtch1*/+ and wild-type control mice (Fig. 3 and see Table S1 in the supplementary material). We detected no change in ER or PR expression between wild-type and either *MMTV-SmoM2* or *ΔPtch1*/+ mice, but detected a significant increase in BrdU incorporation in both *MMTV-SmoM2* (4.4%) and *ΔPtch1*/+ mice (11.3%) relative to wild-type age-matched littermate controls (~0.6%) (Fig. 3, A versus C,E). Elevated BrdU incorporation rates in *MMTV-SmoM2* glands were corroborated by staining for the proliferation marker Ki67 (Mki67 – Mouse Genome Informatics), which was detected in just 6.2% of wild-type cells (Fig. 3A, inset), but in 31.3% of cells in *MMTV-SmoM2* glands (Fig. 3C, inset, and see Table S1 in the supplementary material).

Because the *MMTV-SmoM2* mutant did not recapitulate the *ΔPtch1*/+ phenotype, we expected to observe a compensatory increase in cell death to offset increased proliferation. Wild-type glands showed low levels of cleaved caspase-3 staining (<1%) (Fig. 3B). Contrary to expectations, *MMTV-SmoM2* mice did not show increased caspase-3-mediated apoptosis (Fig. 3D). Glands from *ΔPtch1*/+ mice also showed no change in cleaved caspase-3 expression as a percentage of total epithelial cells (Fig. 3F). Thus, the reason proliferating cells accumulate in glands of *ΔPtch1*/+ mice, but do not accumulate in glands of *MMTV-SmoM2* mice, remains unclear but may be due to non-caspase-3-mediated apoptosis or autophagy.

MMTV-SmoM2 transgene expression and proliferation do not colocalize

The observation that SMO expression was limited, yet morphological defects and expression of proliferation markers were widespread, led us to question to what degree transgene expression correlated with proliferation and hormone receptor status. We conducted dual immunofluorescence staining for SMO, Ki67, and ER, and quantified co-expression in pairwise combinations. Overall, SMO was expressed in 5.7% of all epithelial cells, whereas Ki67 was expressed in 31.3% of epithelial cells. However, SMO and Ki67 did not colocalize (Fig. 4A). We also found that SMO expression did not colocalize with ER (Fig. 4B), with 33.0% of cells showing ER expression exclusively. Unlike wild-type glands, ER and Ki67 colocalized at a low, but measurable, frequency (1.0%) in glands of transgenic mice (Fig. 4C, and see Table S1 in the supplementary material). Proliferation in ER^+ cells was confirmed by co-staining for ER and BrdU (Fig. 4C, inset).

MMTV-SmoM2 mice show altered epithelial cell differentiation

Keratin 6 (CK6; KRT6), a marker of primitive progenitor cells (Grimm et al., 2006; Stingl et al., 2005), is expressed primarily in ER^+ cells in the body cell layer of the TEB, and only rarely in differentiated ducts of mature glands (Grimm et al., 2006). As expected, in mature ducts of 10-week-old wild-type mice, expression of SMO was undetectable and CK6 was observed infrequently (7.5%), and at very low levels (see Table S1 in the supplementary material). However, in 10-week-old *MMTV-SmoM2* mice, CK6 expression was readily detectable in ~20% of epithelial cells (Fig. 4D,E). Co-staining of CK6 and ER demonstrated that the majority of $CK6^+$ cells (82.0%) were also ER^+ (Fig. 4D). There was no colocalization of SMO with CK6 (Fig. 4E with inset). Thus, the *MMTV-SmoM2* transgene was expressed to detectable levels only in non-proliferative ER^- $CK6^-$ cells.

MMTV-SmoM2 increases the proportion of mammosphere-forming cells in mammary glands of transgenic mice in vivo

To determine whether *MMTV-SmoM2* transgenic mice showed a change in the frequency of stem and progenitor cell types relative to wild-type controls, we conducted primary mammosphere-formation assays (Dontu et al., 2003; Dontu and Wicha, 2005). In four of five independent, paired, primary cell preparations, cells derived from *MMTV-SmoM2* mice showed a ~2-fold increase in the percentage of cells capable of forming primary mammospheres (mean raw value=0.76%) relative to cells isolated from wild-type littermate control mice (mean raw value=0.38%) (P=0.02, paired t-test) (Fig. 5A,B). There were no differences in mammosphere size or shape between the two genotypes (Fig. 5C).

To verify that primary mammospheres contained regenerative mammary epithelial stem cells, we transplanted single mammospheres derived from wild-type and *MMTV-SmoM2* mice into contralateral cleared fat pads of 3-week-old host mice. Mammospheres derived from both genotypes showed regenerative potential, with 2 out of 13 (15%) wild-type mammospheres (Fig. 5D, left panel), and 5 out of 15 (33%) *MMTV-SmoM2* mammospheres (Fig. 5D, right panel), capable of regenerating ductal trees. These

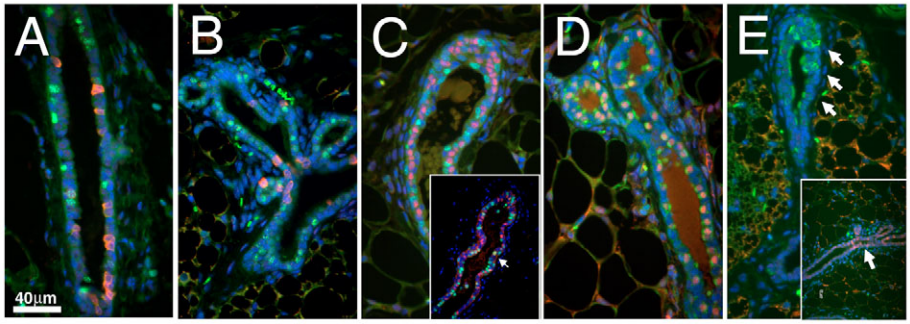

Fig. 4. Dual immunofluorescence analysis of *MMTV-SmoM2* mice at 10 weeks of age. (**A**) SMO-Ki67 showing no colocalization. (**B**) SMO-ER showing no colocalization. (**C**) ER-Ki67 showing low frequency colocalization, confirmed by BrdU-ER dual staining (inset, arrowhead). (**D**) ER-CK6 showing high frequency colocalization. (**E**) Duct showing ectopic CK6 expression (arrowheads), but no detectable SMO expression. (Inset) A region of high SMO expression lacking CK6 expression (arrowhead).

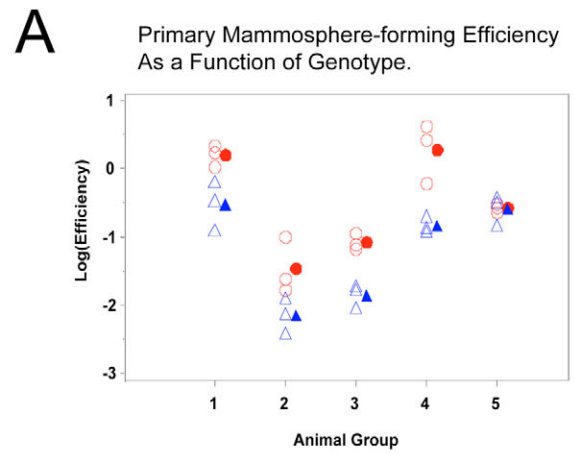

B

T-Tests

Difference	*DF*	*t Value*	*Pr > |t|*
SMO - WT	**4**	**3.67**	**0.0214**

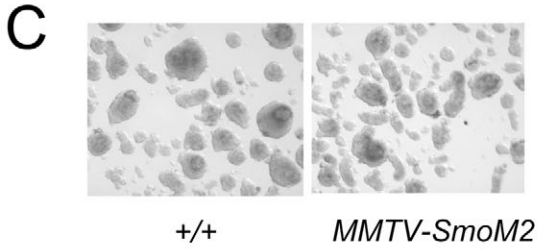

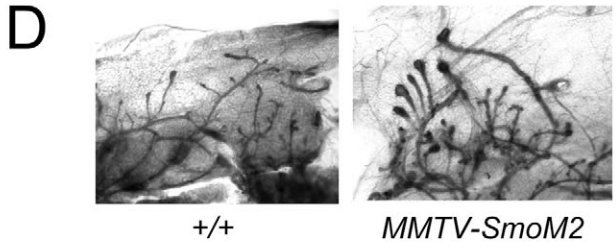

E

	Genotype of epithelial cell donor			
	Wild type		*MMTV-SmoM2*	
Number of cells injected	Take rate	% fat pad filled	Take rate	% fat pad filled
1000	100% (4/4)	87.5 ±15.0	75% (3/4)	90 ±10.0
500	100% (10/10)	95 ±8.5	90% (9/10)	90 ±14.1
200	63% (5/8)	52 ±35.6	63% (5/8)	78 ±38.3
100	65% (11/17)	80 ±16.7	47% (8/17)	53.3 ±29.7
50	47% (7/15)	80 ±27.7	13% (2/15)	50 ±28.3
25	27% (4/15)	20 ±14.1	7% (1/15)	5 ±0.0
Regenerative stem cell frequency (upper and lower limits)	1/106 cells (1/72-1/156)		1/255 cells (1/166-1/390)	

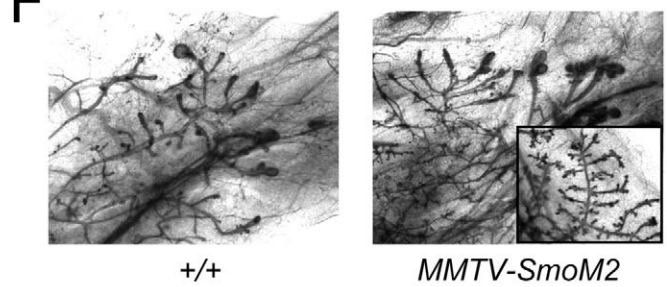

Fig. 5. Effect of *MMTV-SmoM2* on mammosphere formation and regeneration of the mammary gland. (**A**) Pairwise comparison of log-transformed mammosphere-formation efficiency values for five paired sets of primary epithelial cell preparations. *MMTV-SmoM2* cells showed a 2-fold increase in mammosphere-forming efficiency relative to wild-type cells in four of the five sample pairs. Key to symbols: open circles, *MMTV-SmoM2*; red filled circles, *MMTV-SmoM2* average; open trianges, wild type; blue filled triangles, wild-type average. (**B**) Statistical evaluation of mammosphere-forming efficiency as a function of genotype, including all five paired samples shown in A. (**C**) Photomicrographs of representative mammospheres from wild-type and *MMTV-SmoM2* mice. (**D**) Photomicrographs of representative outgrowths of transplanted mammospheres derived from wild-type and *MMTV-SmoM2* mice. (**E**) Limiting-dilution transplantation analysis as a function of genotype. (**F**) Photomicrographs of representative outgrowths from limiting-dilution transplantations (100 cells) derived from wild-type and *MMTV-SmoM2* mice, respectively. Inset shows a strongly affected outgrowth with increased side budding and branching.

regeneration frequencies were not statistically different from one another (P=0.40, Fisher's exact test). Duct morphology in *MMTV-SmoM2* outgrowths was consistently altered as compared with wild type in a manner consistent with the phenotype observed in intact mice.

MMTV-SmoM2 transgene expression decreases the frequency of regenerative stem cells in vivo

Because mammosphere-formation assays are an indirect measure of the frequency of stem cells (e.g. of those with multi-lineage differentiation capacity), and because mammospheres can also be derived from lineage-restricted cell types (e.g. from luminal-only and myoepithelial-only progenitor cells), it was possible that the 2-fold increase in mammosphere-forming efficiency in cells derived from *MMTV-SmoM2* mice might not be due to an increased proportion of regenerative stem cells in vivo, but rather to an increase in the survival (or activity) of other mammosphere-initiating cell types under anchorage-independent growth conditions. To address this possibility, we conducted limiting-dilution transplantation analysis designed to detect differences in the proportion of cells with regenerative capacity directly (Fig. 5E).

For both genotypes, as few as 25 cells were capable of regenerating ductal trees. However, the rate of successful transplantation ('take rate') was lower in cells derived from *MMTV-SmoM2* mice when fewer than 200 cells per gland were injected. Using a single-hit Poisson distribution model we estimate the frequency of regenerative stem cells in wild-type epithelium is 1 stem cell per 106 cells (Fig. 5E). The frequency of regenerative stem cells in *MMTV-SmoM2* epithelium was decreased ~2.5-fold, to 1 stem cell per 255 cells. Again, duct morphology in *MMTV-SmoM2* outgrowths was consistently altered as compared with wild type (Fig. 5F).

Hedgehog signaling is altered at high frequency in human breast cancer

To evaluate a potential role for PTCH1 and SMO in human breast cancer, we conducted an immunohistochemical study for expression of PTCH1 and SMO in a panel of normal, ductal carcinoma in situ

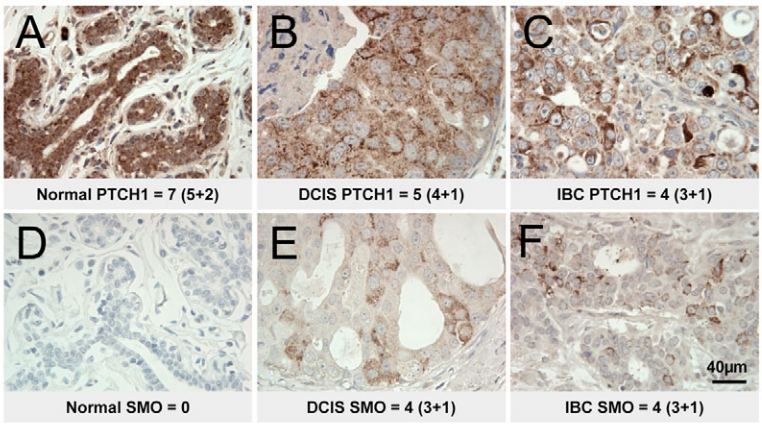

G

	SMO						PTCH1					
Tissue type	N	Mean	SD	Median	Min.	Max.	N	Mean	SD	Median	Min.	Max.
Normal (N)	7	0	0	0	0	0	17	6.76	0.56	7	5	7
DCIS (D)	167	2.57	1.51	3	0	5	172	5.50	1.55	6	0	8
IBC (I)	143	1.76	1.88	2	0	5	142	4.72	1.93	5	0	8

Wilcoxon rank-sum test for total scores

SMO	PTCH1
p=0.0003, N vs. D	p<0.0001, N vs. D
p=0.0163, N vs. I	p<0.0001, N vs. I
p=0.0003, D vs. I	p=0.0001, D vs. I

Fig. 6. PTCH1 and SMO protein expression in human breast cancer. Representative expression patterns are shown with total immunohistochemical score for the sample, with the proportion and intensity scores in parentheses. PTCH1 is readily detectable in normal breast epithelium and isolated stromal cells (**A**), but shows a relative loss in the epithelium in DCIS (**B**) and IBC (**C**) (P<0.0001). SMO expression is undetectable in normal breast (**D**), but is detectable in the cytoplasm in ~70% of DCIS (**E**) and ~30% of IBC (**F**) (P<0.0001). (**G**) Average total IHC scores for SMO and PTCH1 in clinical samples of human breast.

(DCIS), and invasive breast cancer (IBC) samples (Fig. 6). PTCH1 was detectable throughout the epithelium (Fig. 6A), and in isolated stromal cells of the normal breast. By contrast, PTCH1 expression was decreased or absent in ~50% of DCIS (Fig. 6B) and IBC (Fig. 6C). Conversely, SMO was undetectable in normal breast (Fig. 6D), but ectopically expressed in ~70% of DCIS and ~30% of IBC (Fig. 6E,F). For both proteins, total scores between DCIS and IBC were significantly different from each other (SMO, P=0.0003; PTCH1, P=0.0001; Wilcoxon rank-sum test) (Fig. 6G). By Spearman rank correlation analysis, expression of neither PTCH1 nor SMO correlated with histological grade (DCIS only), nor with the expression of any of the clinically-relevant markers tested. PTCH1 expression was not significantly correlated with SMO expression in either DCIS or IBC.

SMO-positive cells are rarely proliferative in human breast cancer

To explore the relationship between PTCH1 or SMO expression and proliferation in human breast cancers, we conducted dual immunofluorescence analysis of PTCH1-Ki67, and of SMO-Ki67, in both DCIS (Fig. 7A-C,G,H) and IBC (Fig. 7D-F,I,J). Lesions in which PTCH1 expression was low to undetectable showed varying degrees of Ki67 staining (Fig. 7A,D). In tumors expressing PTCH1 (Fig. 7B,C,E,F), there was extensive colocalization with the Ki67 proliferation marker. However, in tumors expressing SMO (Fig. 7G-J), SMO expression rarely colocalized with the Ki67 proliferation marker (Fig. 7K).

DISCUSSION

In this paper, we show that expression of constitutively activated human SMO (SmoM2) under the control of the MMTV promoter in transgenic mice leads to ductal dysplasias distinct from those caused by Δ*Ptch1* heterozygosity, despite increased proliferation in both models. SMO expression rarely colocalized with the Ki67 proliferation marker, and activation was not sufficient to cause tumors at high frequency. SMO activation led to altered differentiation, as well as to enhanced primary mammosphere-forming efficiency. However, limiting-dilution transplantation analysis showed a decrease in the frequency of regenerative stem cells in *MMTV-SmoM2* epithelium relative to wild type. In human clinical samples, hedgehog network gene expression is altered frequently, and early, in breast cancer development. As in *MMTV-SmoM2* mice, SMO rarely colocalized with Ki67 in breast tumors. Taken together, these data are consistent with our model that hedgehog signaling must be prevented in mature ducts of virgin mice, and suggest that it is also normally inactive in mature ducts in humans. Thus, ectopic hedgehog signaling could contribute to early breast cancer development by stimulating proliferation, and by increasing the pool of division-competent cells capable of anchorage-independent growth.

In light of our transplantation results published previously (Lewis et al., 1999), failure of *MMTV-SmoM2* to recapitulate the *ΔPtch1/+* hyperplastic phenotype was not entirely unexpected. In these experiments, the *ΔPtch1/+* phenotype could be partially

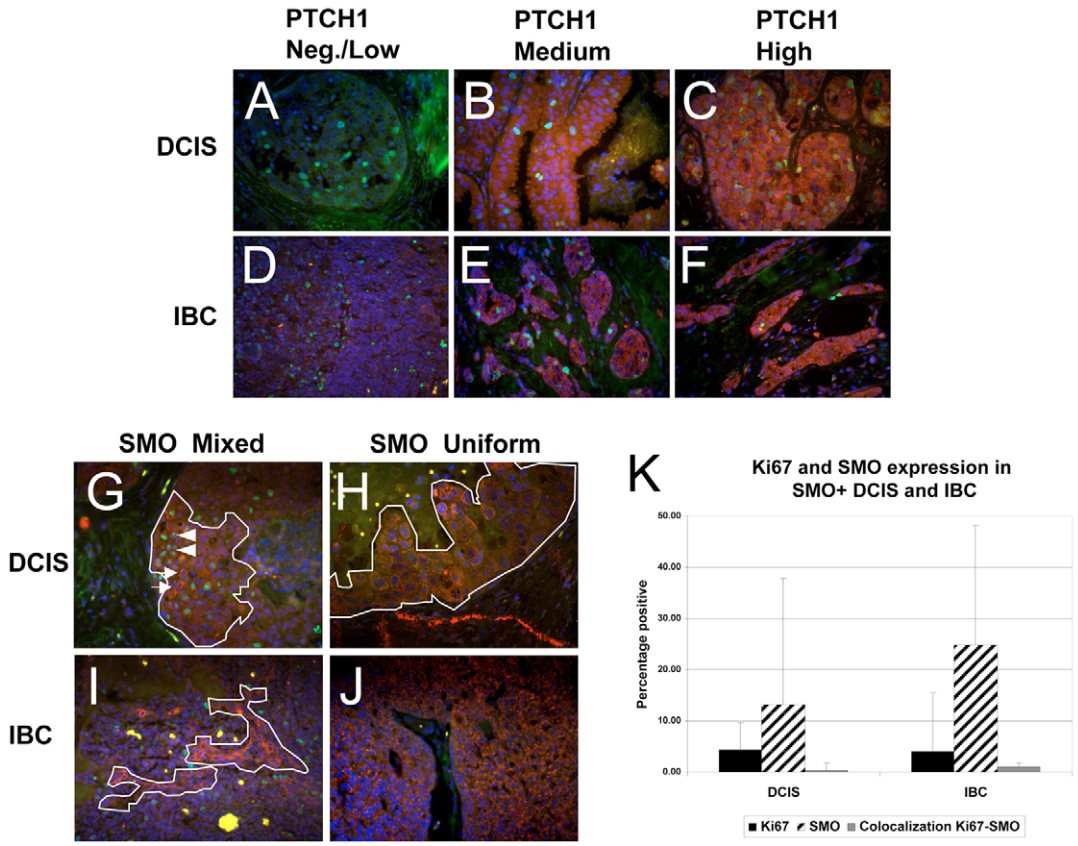

Fig. 7. Dual immunofluorescence analysis of PTCH1-positive and SMO-positive human DCIS and IBC. (**A-F**) PTCH1-Ki67 in DCIS and IBC. Representative staining patterns are shown that indicate extensive colocalization of PTCH1 with Ki67 in those samples expressing detectable PTCH1. (**G-J**) SMO-Ki67 in DCIS and IBC. Representative staining patterns are shown that indicate rare colocalization of SMO with Ki67 in those samples expressing detectable SMO. Arrows and arrowheads in G indicate SMO^+ cells and $Ki67^+$ cells, respectively. (**K**) Quantitative analysis of SMO-Ki67 colocalization in DCIS and IBC.

recapitulated, but only when the entire mammary gland was transplanted – transplantation of epithelial fragments into cleared fat pads of wild-type mice did not lead to ductal dysplasia. These results led to the interpretation that the *ΔPtch1/+* phenotype was due primarily to loss-of-function in mammary stroma. Since the *MMTV-SmoM2* transgene is expressed selectively in the mammary epithelium, stromal activation of hedgehog signaling was not tested here. Thus, the two models are not directly comparable. Regardless of these differences, our results clearly demonstrate that *ΔPtch1* heterozygosity is not functionally equivalent to SMO activation solely in mammary epithelium.

In 10-week-old *MMTV-SmoM2* mice, we demonstrate altered gland morphology in whole-mount preparations, as well as widespread changes in marker expression (Ki67, BrdU incorporation, and CK6) throughout histological preparations of affected glands. However, only ~5.7% of all epithelial cells expressed detectable levels of SMO protein. There are at least three possible interpretations of these results.

First, the simplest interpretation is that SMO is, in fact, only expressed and active in a small percentage of cells in *MMTV-SmoM2* mice. This interpretation then leads to the intriguing hypothesis that SMO activity in these few cells promotes persistence of ER^+CK6^+ cells, and stimulates proliferation indirectly via an undefined paracrine signaling factor (or factors). We are currently testing this hypothesis in a series of in vitro cell mixing and in vivo transplantation experiments, similar to those used recently to demonstrate paracrine signaling functions for the estrogen and progesterone receptors during mammary gland development (Brisken et al., 1998; Mallepell et al., 2006). In addition, we are using alternative models in which SMO activity can be manipulated in vivo (Du et al., 2006; Jeong et al., 2004).

A second possibility is that SMO is expressed and active in greater than 5.7% of cells, but that SMO protein expression is below the limit of detection. Indeed, available antibodies must be used at relatively high concentrations and fail to detect SMO in some tissues known to have hedgehog signaling activity (e.g. E14 embryo, hair follicle, colon) (not shown). This possibility cannot be excluded given currently available reagents. However, if true, this interpretation requires that low-level activity is not sufficient to induce expression of PTCH1 in most cells (Hooper and Scott, 2005) (Fig. 2 and see Fig. S1 in the supplementary material).

A third interpretation is that the primary effect of ectopic SMO expression occurs in, or near, the TEB and leads to a permanent alteration in cell fate. This would require that the permanent alteration leads to inactivation of the MMTV promoter, such that it is no longer expressed. This possibility is being addressed using alternative models in which SMO activity can be controlled in a temporally-regulated manner (Du et al., 2006; Jeong et al., 2004).

With respect to normal mammary development, our data and those of Liu et al. (Liu et al., 2006) are consistent with our working model in which hedgehog signaling may be active in the growing TEB, but signaling is normally absent from mature ducts of wild-type mice (Lewis and Veltmaat, 2004; Lewis and Visbal, 2007). Absence of activated hedgehog signaling in mature ducts is supported by reduced levels of *Ptch1* mRNA in differentiated ducts relative to the TEB, the lack of detectable SMO protein expression, and the failure to detect Gli gene function in mammary epithelium of postnatal animals (Hatsell and Cowin, 2006; Lewis et al., 2001; Lewis and Veltmaat, 2004). However, the definitive experiments required to determine whether active hedgehog signaling functions in the epithelium during postnatal ductal development have never been performed (Lewis and Visbal, 2007). We are currently analyzing conditional null mutants of both *Ptch1* and *Smo*, which should allow us to test our model conclusively (Ellis et al., 2003; Long et al., 2001).

Mammosphere-formation assays are a powerful new addition to our experimental arsenal for the evaluation of stem and progenitor cell types (Dontu et al., 2003; Youn et al., 2005). However, an important caveat to this assay is the fact that not all mammospheres are derived from regenerative stem cells. Using normal human mammary epithelial cells, some mammospheres are derived from multipotent cells, giving rise to both myoepithelial and luminal cell types upon differentiation in culture. These multipotent mammosphere-initiating cells are tacitly assumed to represent regenerative stem cells. Other mammospheres are derived from self-renewing, lineage-restricted progenitors that are capable of differentiating into myoepithelial-only or luminal-only cell colonies. These mammosphere-initiating cells are thought to represent more-differentiated downstream progenitor cells that should not have regenerative potential. Unfortunately, the regenerative potential of either of these populations cannot be formally tested with existing xenograft technology; thus, the frequency of regenerative stem cells in the normal human mammary gland is not known.

Fortunately, the technical limitations inherent in the use of human mammary epithelial cells do not apply to mouse mammary epithelial cells, where it is possible to assay directly whether mammospheres contain (and are therefore likely to be derived from) regenerative stem cells using single mammosphere transplantation, as well as to estimate directly the proportion of regenerative stem cells present in the mammary gland. According to our results using mouse cells, the proportion of mammospheres containing regenerative stem cells is approximately 15-33%. Thus, the remaining 67-85% of mammospheres are likely to be derived from downstream progenitor cell types lacking regenerative potential. To our knowledge, these are the first data to demonstrate directly the regenerative capacity of single mammospheres.

Given that at least three sub-populations of mammosphere-initiating cells are known to exist in humans, and that similar subsets of cells are likely to exist in mice, we do not believe that our mammosphere-formation results showing a ~2-fold increase in mammosphere-formation efficiency, and our limiting-dilution transplantation data showing a ~2.5-fold decrease in the frequency of regenerative stem cells in *MMTV-SmoM2* mice, are contradictory. Our interpretation of the mammosphere-formation versus limiting-dilution transplantation data is that expression of *MMTV-SmoM2* may favor differentiation of stem cells into downstream proliferating progenitor cell pools. From our in vivo gene expression data, we present evidence that we increase a pool of proliferative $ER^{-}CK6^{-}$ cells, as well as a pool of $ER^{+}CK6^{+}$ cells that divides at a lower frequency. These proliferating cell pools may be capable of mammosphere-formation, but be incapable of regenerating a mammary gland upon transplantation.

A potential limitation of secondary mammosphere-formation assays for the evaluation of changes in self-renewal capacity in MMTV transgenic mice was revealed. In our hands, transgene expression was not detectable in primary mammospheres by immunofluorescence (not shown). Because of this, secondary mammosphere-formation assays to test for changes in stem cell self-renewal as a consequence of transgene expression during primary mammosphere culture were not considered reliable. Thus, it is difficult to compare our mouse mammosphere-formation data directly with those of Liu et al. (Liu et al., 2006), who demonstrated increased primary and secondary mammosphere formation in response to treatment with recombinant SHH ligand using human cells. We are currently repeating these experiments using mouse primary mammary epithelial cells to reconcile these two datasets.

With respect to human breast disease, there are some data to suggest a role for altered hedgehog signaling in mammary cancer. An early study found *Ptch1* mutations in two of seven human breast cancers (Xie et al., 1997). Additionally, a *Ptch1* polymorphism was linked to increased breast cancer risk associated with oral contraceptive use (Chang-Claude et al., 2003). More recently, array comparative genomic hybridization (CGH) analyses indicate that genomic loss at the *Ptch1* locus was the fourth most commonly detected change among the tumor suppressor genes identified in the study, occurring in 19% of human breast cancers and in 33% of breast cancer cell lines (Naylor et al., 2005). However, no mutations in other network components have been identified in breast cancer (Vorechovsky et al., 1999). A recent immunohistochemical staining study suggested that hedgehog signaling is activated in a majority of human invasive breast cancers based on ectopic expression of PTCH1 and nuclear GLI1 (Kubo et al., 2004). However, two other studies show loss of PTCH1 in many cases, perhaps owing, in part, to promoter methylation (Kubo et al., 2004; Mukherjee et al., 2006; Wolf et al., 2007). Finally, the hedgehog signaling inhibitor cyclopamine inhibited growth of some breast cell lines in vitro (Kubo et al., 2004; Mukherjee et al., 2006). However, the specificity of cyclopamine at the doses required for growth inhibition remains an open question (Mukherjee et al., 2006).

Our data showing loss of PTCH1 protein expression in ~50% of DCIS and IBC are most consistent with the array CGH results, as well as with recent immunostaining and methylation data (Kubo et al., 2004; Mukherjee et al., 2006; Wolf et al., 2007), but differ significantly from the immunohistochemical study by Kubo et al. (Kubo et al., 2004). The reason for the discrepancies among these studies is unclear, but may be related to the different antigen retrieval strategies used. To date, the preponderance of the data indicates that PTCH1 is lost or reduced in ~50% of all breast cancers. Altered SMO expression in human breast cancer has not been demonstrated previously. Given that SMO was not detectable in normal human or mouse tissue, but was readily detectable in *MMTV-SmoM2* mice, we are confident of the specificity of the two antibodies used.

Our observation that SMO protein expression does not colocalize frequently with proliferation markers in either the *MMTV-SmoM2* mouse model or in human breast tumors was unexpected. These observations must be reconciled with data suggesting a direct role for hedgehog signaling in normal human stem cell self-renewal (Liu et al., 2006), and with reports that hedgehog signaling activation appears to increase proliferation directly in other cell types (e.g. Detmer et al., 2005; Hutchin et al., 2005; MacLean and Kronenberg, 2005; Palma et al., 2005). In any case, the similarity in staining

patterns of SMO relative to proliferation markers in both the mouse and human models suggests that our *MMTV-SmoM2* transgenic model reflects important aspects of human breast tumor biology, and that it will therefore be a useful model for studying the underlying mechanism of hedgehog network regulation of stem/progenitor cell behavior in mammary gland development and breast cancer.

The authors are very grateful to Drs Jeffrey Rosen, Gary Chamness and Yi Li for critical comments on the manuscript. This work was supported by grants from the National Institute of Health P01-CA30195 (to M.T.L.) and P50-CA58183 (to D.C.A.), and from the Department of Defense (IDEA) 17-00-1-0477 (to M.T.L.).

Supplementary material

Supplementary material for this article is available at http://dev.biologists.org/cgi/content/full/134/6/1231/DC1

References

Allred, D. C., Harvey, J. M., Berardo, M. and Clark, G. M. (1998). Prognostic and predictive factors in breast cancer by immunohistochemical analysis. *Mod. Pathol.* **11**, 155-168.

Bonnefoix, T., Bonnefoix, P., Verdiel, P. and Sotto, J. J. (1996). Fitting limiting dilution experiments with generalized linear models results in a test of the single-hit Poisson assumption. *J. Immunol. Methods* **194**, 113-119.

Briscoe, J. and Therond, P. (2005). Hedgehog signaling: from the Drosophila cuticle to anti-cancer drugs. *Dev. Cell* **8**, 143-151.

Brisken, C., Park, S., Vass, T., Lydon, J. P., O'Malley, B. W. and Weinberg, R. A. (1998). A paracrine role for the epithelial progesterone receptor in mammary gland development. *Proc. Natl. Acad. Sci. USA* **95**, 5076-5081.

Chang-Claude, J., Dunning, A., Schnitzbauer, U., Galmbacher, P., Tee, L., Wjst, M., Chalmers, J., Zemzoum, I., Harbeck, N., Pharoah, P. D. et al. (2003). The patched polymorphism Pro1315Leu (C3944T) may modulate the association between use of oral contraceptives and breast cancer risk. *Int. J. Cancer* **103**, 779-783.

Chao, M. V. (2003). Dependence receptors: what is the mechanism? *Sci. STKE* **2003**, PE38.

Chen, M. S., Woodward, W. A., Behbod, F., Peddibhotla, S., Alfaro, M. P., Buchholz, T. A. and Rosen, J. M. (2007). Wnt/beta-catenin mediates radiation resistance of stem cell antigen-1 positive progenitors in an immortalized mammary gland cell line. *J. Cell Sci.* **120**, 468-477.

Cohen, M. M., Jr (2003). The hedgehog signaling network. *Am. J. Med. Genet. A* **123**, 5-28.

Daniel, C. W. and Silberstein, G. B. (1987). Developmental biology of the mammary gland. In *The Mammary Gland* (ed. M. C. Neville and C. W. Daniel), pp. 3-36. New York: Plenum.

Deome, K. B., Faulkin, L. J., Jr, Bern, H. A. and Blair, P. B. (1959). Development of mammary tumors from hyperplastic alveolar nodules transplanted into gland-free mammary fat pads of female C3H mice. *Cancer Res.* **19**, 515-520.

Detmer, K., Thompson, A. J., Garner, R. E., Walker, A. N., Gaffield, W. and Dannawi, H. (2005). Hedgehog signaling and cell cycle control in differentiating erythroid progenitors. *Blood Cells Mol. Dis.* **34**, 60-70.

Dontu, G. and Wicha, M. S. (2005). Survival of mammary stem cells in suspension culture: implications for stem cell biology and neoplasia. *J. Mammary Gland Biol. Neoplasia* **10**, 75-86.

Dontu, G., Abdallah, W. M., Foley, J. M., Jackson, K. W., Clarke, M. F., Kawamura, M. J. and Wicha, M. S. (2003). In vitro propagation and transcriptional profiling of human mammary stem/progenitor cells. *Genes Dev.* **17**, 1253-1270.

Du, Z., Podsypanina, K., Huang, S., McGrath, A., Toneff, M. J., Bogoslovskaia, E., Zhang, X., Moraes, R. C., Fluck, M., Allred, D. C. et al. (2006). Introduction of oncogenes into mammary glands in vivo with an avian retroviral vector initiates and promotes carcinogenesis in mouse models. *Proc. Natl. Acad. Sci. USA* **103**, 17396-17401.

Ellis, T., Smyth, I., Riley, E., Graham, S., Elliot, K., Narang, M., Kay, G. F., Wicking, C. and Wainwright, B. (2003). Patched 1 conditional null allele in mice. *Genesis* **36**, 158-161.

Gallego, M. I., Beachy, P. A., Hennighausen, L. and Robinson, G. W. (2002). Differential requirements for shh in mammary tissue and hair follicle morphogenesis. *Dev. Biol.* **249**, 131-139.

Grimm, S. L., Bu, W., Longley, M. A., Roop, D. R., Li, Y. and Rosen, J. M. (2006). Keratin 6 is not essential for mammary gland development. *Breast Cancer Res.* **8**, R29.

Guerrero, I. and Ruiz i Altaba, A. (2003). Development. Longing for ligand: hedgehog, patched, and cell death. *Science* **301**, 774-776.

Harvey, J. M., Clark, G. M., Osborne, C. K. and Allred, D. C. (1999). Estrogen receptor status by immunohistochemistry is superior to the ligand-binding assay for predicting response to adjuvant endocrine therapy in breast cancer. *J. Clin. Oncol.* **17**, 1474-1481.

Hatsell, S. J. and Cowin, P. (2006). Gli3-mediated repression of Hedgehog targets is required for normal mammary development. *Development* **133**, 3661-3670.

Hooper, J. E. and Scott, M. P. (2005). Communicating with Hedgehogs. *Nat. Rev. Mol. Cell Biol.* **6**, 306-317.

Hutchin, M. E., Kariapper, M. S., Grachtchouk, M., Wang, A., Wei, L., Cummings, D., Liu, J., Michael, L. E., Glick, A. and Dlugosz, A. A. (2005). Sustained Hedgehog signaling is required for basal cell carcinoma proliferation and survival: conditional skin tumorigenesis recapitulates the hair growth cycle. *Genes Dev.* **19**, 214-223.

Jeong, J., Mao, J., Tenzen, T., Kottmann, A. H. and McMahon, A. P. (2004). Hedgehog signaling in the neural crest cells regulates the patterning and growth of facial primordia. *Genes Dev.* **18**, 937-951.

Kubo, M., Nakamura, M., Tasaki, A., Yamanaka, N., Nakashima, H., Nomura, M., Kuroki, S. and Katano, M. (2004). Hedgehog signaling pathway is a new therapeutic target for patients with breast cancer. *Cancer Res.* **64**, 6071-6074.

Lewis, M. T. and Veltmaat, J. M. (2004). Next stop, the twilight zone: hedgehog network regulation of mammary gland development. *J. Mammary Gland Biol. Neoplasia* **9**, 165-181.

Lewis, M. T. and Visbal, A. P. (2007). The Hedgehog signaling network, mammary stem cells, and breast cancer: connections and controversies. *Ernst Schering Res. Found. Workshop*. (in press).

Lewis, M. T., Ross, S., Strickland, P. A., Sugnet, C. W., Jimenez, E., Scott, M. P. and Daniel, C. W. (1999). Defects in mouse mammary gland development caused by conditional haploinsufficiency of Patched-1. *Development* **126**, 5181-5193.

Lewis, M. T., Ross, S., Strickland, P. A., Sugnet, C. W., Jimenez, E., Hui, C. and Daniel, C. W. (2001). The Gli2 transcription factor is required for normal mouse mammary gland development. *Dev. Biol.* **238**, 133-144.

Liu, S., Dontu, G., Mantle, I. D., Patel, S., Ahn, N. S., Jackson, K. W., Suri, P. and Wicha, M. S. (2006). Hedgehog signaling and Bmi-1 regulate self-renewal of normal and malignant human mammary stem cells. *Cancer Res.* **66**, 6063-6071.

Livak, K. J. and Schmittgen, T. D. (2001). Analysis of relative gene expression data using real-time quantitative PCR and the 2(–Delta Delta C(T)) Method. *Methods* **25**, 402-408.

Long, F., Zhang, X. M., Karp, S., Yang, Y. and McMahon, A. P. (2001). Genetic manipulation of hedgehog signaling in the endochondral skeleton reveals a direct role in the regulation of chondrocyte proliferation. *Development* **128**, 5099-5108.

MacLean, H. E. and Kronenberg, H. M. (2005). Localization of Indian hedgehog and PTH/PTHrP receptor expression in relation to chondrocyte proliferation during mouse bone development. *Dev. Growth Differ.* **47**, 59-63.

Mallepell, S., Krust, A., Chambon, P. and Brisken, C. (2006). Paracrine signaling through the epithelial estrogen receptor {alpha} is required for proliferation and morphogenesis in the mammary gland. *Proc. Natl. Acad. Sci. USA* **103**, 2196-2201.

Michno, K., Boras-Granic, K., Mill, P., Hui, C. C. and Hamel, P. A. (2003). Shh expression is required for embryonic hair follicle but not mammary gland development. *Dev. Biol.* **264**, 153-165.

Mukherjee, S., Frolova, N., Sadlonova, A., Novak, Z., Steg, A., Page, G. P., Welch, D. R., Lobo-Ruppert, S. M., Ruppert, J. M., Johnson, M. R. et al. (2006). Hedgehog signaling and response to cyclopamine differ in epithelial and stromal cells in benign breast and breast cancer. *Cancer Biol. Ther.* **5**, 674-683.

Naylor, T. L., Greshock, J., Wang, Y., Colligon, T., Yu, Q. C., Clemmer, V., Zaks, T. Z. and Weber, B. L. (2005). High resolution genomic analysis of sporadic breast cancer using array-based comparative genomic hybridization. *Breast Cancer Res.* **7**, R1186-R1198.

Nusse, R. (2003). Wnts and Hedgehogs: lipid-modified proteins and similarities in signaling mechanisms at the cell surface. *Development* **130**, 5297-5305.

Palma, V., Lim, D. A., Dahmane, N., Sanchez, P., Brionne, T. C., Herzberg, C. D., Gitton, Y., Carleton, A., Alvarez-Buylla, A. and Ruiz i Altaba, A. (2005). Sonic hedgehog controls stem cell behavior in the postnatal and adult brain. *Development* **132**, 335-344.

Sakakura, T. (1987). Mammary embryogenesis. In *The Mammary Gland* (ed. M. C. Neville and C. W. Daniel), pp. 37-66. New York: Plenum.

Smith, G. H. (1996). Experimental mammary epithelial morphogenesis in an in vivo model: evidence for distinct cellular progenitors of the ductal and lobular phenotype. *Breast Cancer Res. Treat.* **39**, 21-31.

Stingl, J., Raouf, A., Emerman, J. T. and Eaves, C. J. (2005). Epithelial progenitors in the normal human mammary gland. *J. Mammary Gland Biol. Neoplasia* **10**, 49-59.

Thibert, C., Teillet, M. A., Lapointe, F., Mazelin, L., Le Douarin, N. M. and Mehlen, P. (2003). Inhibition of neuroepithelial patched-induced apoptosis by sonic hedgehog. *Science* **301**, 843-846.

Vorechovsky, I., Benediktsson, K. P. and Toftgard, R. (1999). The patched/hedgehog/smoothened signalling pathway in human breast cancer: no evidence for H133Y SHH, PTCH and SMO mutations. *Eur. J. Cancer* **35**, 711-713.

Williams, J. M. and Daniel, C. W. (1983). Mammary ductal elongation: differentiation of myoepithelium and basal lamina during branching morphogenesis. *Dev. Biol.* **97**, 274-290.

Wolf, I., Bose, S., Desmond, J. C., Lin, B. T., Williamson, E. A., Karlan, B. Y. and Koeffler, H. P. (2007). Unmasking of epigenetically silenced genes reveals DNA promoter methylationand reduced expression of PTCH in breast cancer. *Breast Cancer Res. Treat.* (in press).

Xie, J., Johnson, R. L., Zhang, X., Bare, J. W., Waldman, F. M., Cogen, P. H., Menon, A. G., Warren, R. S., Chen, L. C., Scott, M. P. et al. (1997). Mutations of the PATCHED gene in several types of sporadic extracutaneous tumors. *Cancer Res.* **57**, 2369-2372.

Xie, J., Murone, M., Luoh, S. M., Ryan, A., Gu, Q., Zhang, C., Bonifas, J. M., Lam, C. W., Hynes, M., Goddard, A. et al. (1998). Activating Smoothened mutations in sporadic basal-cell carcinoma. *Nature* **391**, 90-92.

Youn, B. S., Sen, A., Kallos, M. S., Behie, L. A., Girgis-Gabardo, A., Kurpios, N., Barcelon, M. and Hassell, J. A. (2005). Large-scale expansion of mammary epithelial stem cell aggregates in suspension bioreactors. *Biotechnol. Prog.* **21**, 984-993.